The p53-induced factor Ei24 inhibits nuclear import through an importin β–binding–like domain

Kim G. Lieu,[1] Eun-Hee Shim,[2] Jinling Wang,[2] Ravi K. Lokareddy,[3] Tao Tao,[4] Gino Cingolani,[3] Gerard P. Zambetti,[2] and David A. Jans[1]

[1]Department of Biochemistry and Molecular Biology, Monash University, Clayton, Victoria 3800, Australia
[2]Department of Biochemistry, St. Jude Children's Research Hospital, Memphis, TN 38105
[3]Department of Biochemistry and Molecular Biology, Thomas Jefferson University, Philadelphia, PA 19107
[4]Xiamen University School of Life Sciences, Xiamen, Fujian 361005, China

The etoposide-induced protein Ei24 was initially identified as a p53-responsive, proapoptotic factor, but no clear function has been described. Here, we use a nonbiased proteomics approach to identify members of the importin (IMP) family of nuclear transporters as interactors of Ei24 and characterize an IMPβ-binding-like (IBBL) domain within Ei24. We show that Ei24 can bind specifically to IMPβ1 and IMPα2, but not other IMPs, and use a mutated IMPβ1 derivative to show that Ei24 binds to the same site on IMPβ1 as the IMPα IBB.

Ectopic expression of Ei24 reduced the extent of IMPβ1- or IMPα/β1-dependent nuclear protein import specifically, whereas specific alanine substitutions within the IBBL abrogated this activity. Induction of endogenous Ei24 expression through etoposide treatment similarly inhibited nuclear import in a mouse embryonic fibroblast model. Thus, Ei24 can bind specifically to IMPβ1 and IMPα2 to impede their normal role in nuclear import, shedding new light on the cellular functions of Ei24 and its tumor suppressor role.

Introduction

Nuclear protein import is dependent on NLSs, which are recognized by members of the importin (IMP) superfamily of nuclear transport receptors (Poon and Jans, 2005). The best characterized pathway involves the recognition of an NLS-containing cargo by IMPβ1 directly or the IMPα/β1 heterodimer, where IMPα is an adaptor protein (Cingolani et al., 2002; Poon and Jans, 2005). In the absence of IMPβ1, IMPα is "autoinhibited" through an intrinsic NLS within IMPα's IMPβ-binding (IBB) domain, which binds to its NLS binding site (Kobe, 1999; Harreman et al., 2003a,b; Goldfarb et al., 2004). Binding of IMPβ1 to the IBB domain relieves IMPα autoinhibition to permit accessibility to the NLS binding site (Cingolani et al., 1999; Kobe, 1999; Conti and Kuriyan, 2000; Goldfarb et al., 2004). IMPβ1 subsequently mediates passage of the IMPα/β heterodimer–cargo complex through the nuclear envelope–embedded nuclear

pore, before dissociation of the complex in the nucleus upon binding to IMPβ1 of the monomeric guanine nucleotide binding protein Ran in activated GTP-bound form (Poon and Jans, 2005).

Mechanisms of regulation of nuclear protein import, central to signal transduction/transcriptional outcomes in the nucleus, include those mediated by a specialized class of diverse cytoplasmic proteins, negative regulators of nuclear import (NRNIs), which sequester molecules in the cytoplasm to prevent their nuclear import. Cytoplasmic retention of the NLS-containing transcription factors NF-κB and Gli1, for example, is effected by specific NRNIs, such as inhibitor of κBα (IκBα) and suppressor of fused (Su(fu)), respectively, which prevent IMP recognition by NLS masking (Jacobs and Harrison, 1998; Ding et al., 1999; Bergqvist et al., 2006). Analogously, the BRCA1-binding protein BRAP2 (Li et al., 1998) can negatively regulate the nuclear import of different cellular and viral proteins, dependent on phosphorylation flanking the NLS (Fulcher et al., 2010). Finally, a truncated form of IMPα2 ("CanRch1") from

---

The Rockefeller University Press $30.00
J. Cell Biol. Vol. 205 No. 3   301–312
www.jcb.org/cgi/doi/10.1083/jcb.201304055

JCB   301

THE JOURNAL OF CELL BIOLOGY

Figure 1. **Ei24 coprecipitates and colocalizes with specific IMPs and shares homology with the IBB domain of IMPα2.** (A) FLAG-Ei24 expressed in HEK293T cells was immunoprecipitated using anti-FLAG (lane 1) or anti-Ei24 (lane 2) antibodies. Bound proteins were separated by SDS-PAGE, transferred to a nylon membrane, stained with a Sypro Ruby dye, and subsequently analyzed by MALDI-TOF MS. Bands identified as IMPβ1, IMP7, and Ei24 are indicated (see Table S1 for details). (B) Endogenous Ei24 or IgG immunoprecipitates (IP)/input lysates from HEK293T cells were resolved by SDS-PAGE

a human breast cancer line has been reported to inhibit nuclear accumulation of the tumor suppressor p53 (Kim et al., 2000).

Here, we describe the ability of the etoposide-induced protein Ei24 (etoposide-induced mRNA 2.4 kb) to act as an NRNI for the first time. Ei24 is an ER-localized protein (Zhao et al., 2005, 2012) originally identified as a p53-induced pro-apoptotic gene in etoposide-treated NIH3T3 cells (Lehar et al., 1996). It has been shown to be able to bind to the antiapoptotic protein Bcl-2 (Zhao et al., 2005), play a role in autophagy (Tian et al., 2010; Zhao et al., 2012), and induce growth arrest/apoptosis (Gu et al., 2000), but very little is known about how Ei24 may mediate these diverse functions. To address this, we used a nonbiased proteomics approach, identifying members of the IMP superfamily as binding partners of Ei24. We show that Ei24 contains an "IBB-like" (IBBL) domain conferring strong interaction with IMPα2 and IMPβ1 in a similar fashion to the IBB of IMPα2. We also show that Ei24 is able to reduce the nuclear accumulation of IMPα/β1- and IMPβ1-dependent cargoes, dependent on key basic residues within the IBBL domain; induction of endogenous Ei24 expression through etoposide treatment has the same effect. Collectively, the findings indicate that Ei24 is a novel IBBL-containing NRNI, shedding new light on Ei24's various cellular functions.

Results and discussion

Ei24 interacts with specific IMPs and shares homology with IMPα2

Previous studies have implicated Ei24 in growth arrest, apoptosis, and autophagy (Polyak et al., 1997; Gu et al., 2000; Zhao et al., 2005, 2012; Tian et al., 2010). We applied a nonbiased proteomics approach to identify potential interacting proteins of Ei24 from human embryonic kidney HEK293T cells transfected to express FLAG-tagged Ei24 (FLAG-Ei24), subjected to immunoprecipitation (IP) using anti-FLAG or -Ei24 antibodies (Fig. 1 A) with preimmune serum as a control (Fig. S1 A). Mass spectrometric analysis identified Ei24, as well as several other proteins enriched in the anti-FLAG and -Ei24 immunoprecipitates, including the IMPβ superfamily members IMPβ1 and Ran-binding protein 7 (IMP7; Fig. 1 A and Table S1). CoIP of endogenous Ei24 under high stringency conditions followed by Western analysis using specific antibodies confirmed that IMPβ1, IMPα2, and IMP7, but not IMPβ2 or IMPα4, were complexed to Ei24 under physiological conditions (Fig. 1 B and not depicted).

Perusal of the human and mouse Ei24 sequence revealed a conserved, basic 51–amino acid region (Fig. 1 C) with ∼33% similarity to IMPα2's IBB, a highly basic domain that is recognized specifically by IMPβ1 to facilitate formation of the IMPα/β1 heterodimer (Cingolani et al., 1999). We named this

the IBBL domain of Ei24, and first tested whether it can confer binding to IMPβ1 and/or IMPα2 in a similar fashion to the IBB of IMPα. Consistent with this idea, endogenous Ei24 was found to colocalize with IMPβ1, IMPα2, and IMP7, particularly in the perinuclear region of HeLa cells treated with etoposide to up-regulate Ei24 expression (Fig. 1 D; see Fig. S1, C and D, indicating a significant approximately twofold increase in the extent of colocalization, concentrated to a marked extent at the ER). Importantly, proteinase K digestion of preparations of ER from subcellular fractionation experiments of cells expressing N-terminally FLAG-tagged Ei24 indicated that the IBBL was exposed to the cytosol (Fig. S1 B), which is consistent with the idea that Ei24–IMP interaction in the cytoplasm/at the ER may occur under normal physiological conditions.

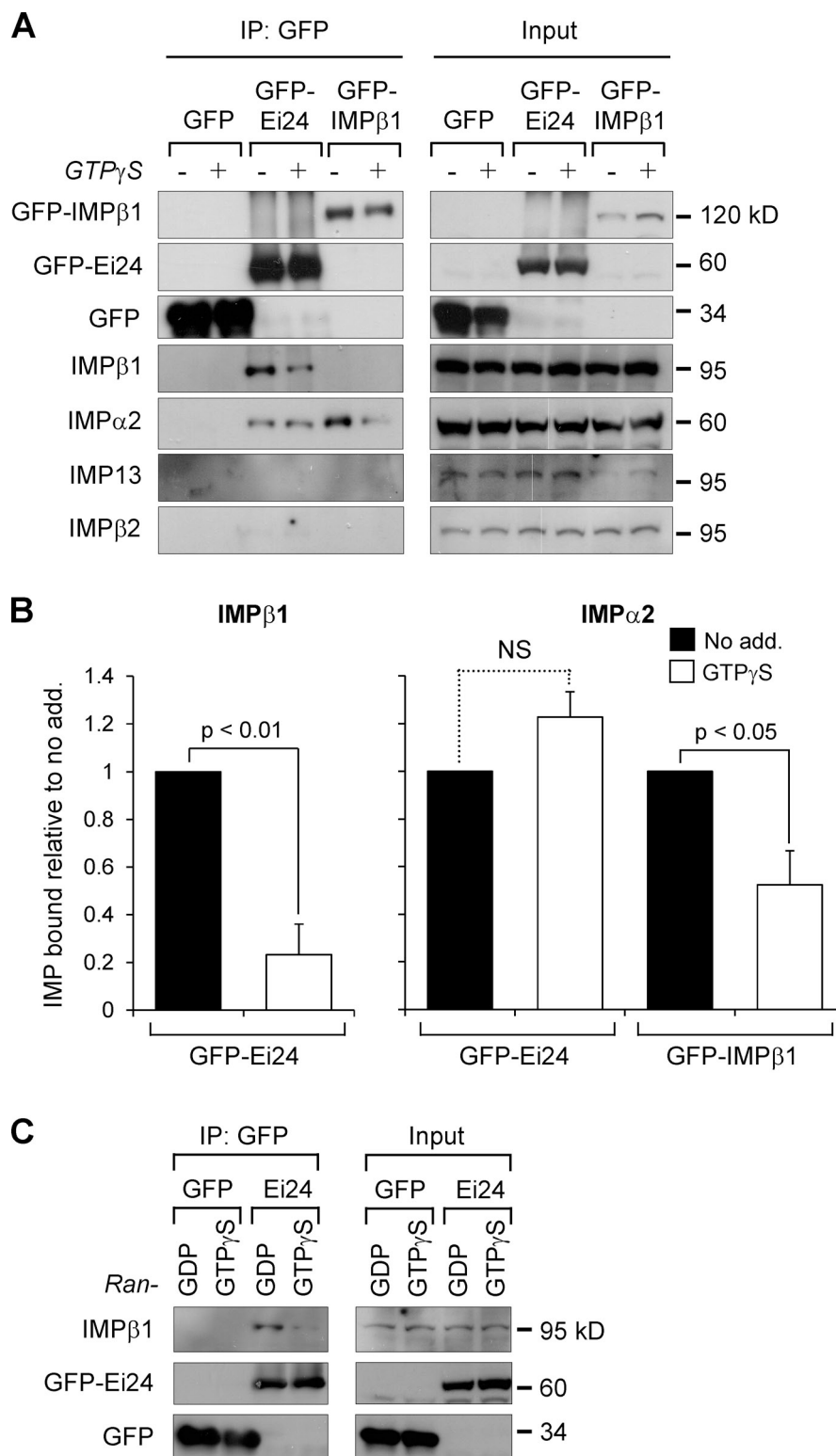### RanGTP can effect IMPβ1-dependent dissociation from Ei24

After IMP-mediated transport into the nucleus, binding of RanGTP to IMPβ1 dissociates the transport complex by displacing IMPα2's IBB from IMPβ1 (Görlich et al., 1996b; Lee et al., 2005). To test if RanGTP can release endogenous IMPβ1 from Ei24, GFP-tagged Ei24 (GFP-Ei24) was immunoprecipitated in the absence or presence of GTPγS, a nonhydrolyzable form of GTP that maintains Ran in the GTP-bound state, followed by Western analysis and densitometry (Fig. 2, A and B). As expected, IMPα2 was coprecipitated with the control protein GFP-IMPβ1 in the absence of GTPγS, but to a significantly (P < 0.05) lower extent in its presence. Importantly, GTPγS decreased GFP-Ei24 binding to IMPβ1 (P < 0.01); similar results were observed upon the addition of recombinant Ran loaded with GTPγS but not GDP to lysates from cells expressing GFP-Ei24 (Fig. 2 C). In contrast to the results for IMPβ1, pull-down of IMPα2 by GFP-Ei24 was unaffected by GTPγS (Fig. 2, A and B), whereas GFP-Ei24 did not coprecipitate other IMPβ homologues such as IMPβ2 or IMP13; GFP alone did not coprecipitate any IMP, which implies that the observed interactions are specific. These results support the idea that RanGTP can inhibit Ei24–IMPβ1 binding, which is consistent with Ei24's IBBL conferring interaction with IMPβ1 in an analogous fashion to the IBB of IMPα.

Ei24 binds to IMPs with high affinity

We next tested whether Ei24's IBBL can bind directly to IMPs in vitro, comparing results to those of CanRch1, a form of IMPα2 truncated at residue 89 that includes the IBB but not the NLS-binding domain (Kim et al., 2000). An AlphaScreen binding assay (Wagstaff and Jans, 2006) was performed using purified bacterially expressed His_6-IMPs, biotinylated GST-CanRch1 and -Ei24N (2–225 aa) proteins (Fig. 3 and Table 1).

before Western analysis using the specific antibodies indicated. (C) Multiple sequence alignment of the human and mouse Ei24 IBBL domains (predicted to form an α-helical structure using Protein Homology/Analogy Recognition Engine version 2.0) together with IMPα2/CanRch1, performed as described in Materials and methods. Numbers indicate the portion of the amino acid residues (single letter code) within the respective proteins. Gray and black shading indicates similar and identical residues, respectively. Sites of targeted mutation in this study are indicated by asterisks. (D) HeLa cells treated with 50 µM etoposide or DMSO vehicle control for 16 h were fixed and immunostained using specific antibodies for endogenous IMPβ1, IMPα2, IMP7, or Ei24, and counterstained with DAPI. Merged images are shown at higher magnification (high mag., bottom panels). Yellow coloration in merged images indicates colocalization; quantitative analysis is presented in Fig. S1, C and D. Bars, 20 µm.

Figure 2. IMPβ1 recognition by Ei24 is inhibited in the presence of GTPγS or recombinant RanGTP. (A) Lysates from HeLa-Bcl$_{XL}$ cells expressing GFP, GFP-Ei24, or GFP-IMPβ1 fusion proteins prepared 20 h after transfection were subjected to IP with GFP-Trap resin in the absence or presence of 1.7 mM GTPγS. Western analysis was performed on input and immuno-precipitates (IP: GFP) using the specific antibodies indicated. (B) Densitometric analysis was performed on images such as those shown in A for binding of endogenous IMPβ1 (left) and IMPα2 (right) to GFP-Ei24 or GFP-IMPβ1, as indicated. Pooled results ($n \geq 2$) representing the mean ± SD (error bars) for IMP bound relative to no GTPγS treatment (No add.) are shown; p-values (Student's *t* test) denote significant differences. NS, not significant. (C) Lysates from HeLa-Bcl$_{XL}$ cells expressing GFP-Ei24 or GFP alone were incubated for 20 min with 3 µM recombinant of Ran loaded with GTPγS or GDP, before IP and Western blot analysis as in A.

Ei24 2–225 corresponds to a clinically derived, breast cancer truncated form of Ei24 that lacks the C-terminal 133 residues but retains the IBBL (Gentile et al., 2001).

Ei24N resembled CanRch1 in binding to IMPβ1 with high affinity (∼5 nM); in contrast, a mutant of IMPβ1 unable to bind the IBB ("IBBm," mutated at residues W430/W472/W864; Koerner et al., 2003), showed significantly (P < 0.0001) reduced (>80%) binding to both Ei24N and CanRch1 (Fig. 3), which indicates that the Ei24 IBBL requires the same residues on IMPβ1 for high-affinity binding as those interacting with the prototypical IBB. Ei24N and CanRch1 also bound to IMPα2ΔIBB (truncated form of IMPα2 lacking the IBB) in near identical fashion to IMPβ1 in terms of both maximal binding and K_d (∼4 nM); binding to full-length (FL) IMPα2 wild

A

B-GST-Ei24N

% binding relative to IMPβ1 WT

IMPβ1 WT, K_d=4.8 nM

IMPβ1 IBBm, K_d=ND

B-GST-CanRch1

IMPβ1 WT, K_d=5 nM

IMPβ1 IBBm, K_d=ND

% binding relative to IMPα2ΔIBB

IMPα2ΔIBB, K_d=3.9 nM

IMPα2 WT, K_d=3 nM

IMPα2ΔIBB, K_d=3.6 nM

IMPα2 WT, K_d=5.5 nM

IMP (nM)

B

p < 0.0001   p < 0.0001

% max. binding relative to IMPβ1 WT

WT   IBBm   WT   IBBm
Ei24N   CanRch1

p < 0.001   p < 0.01

% max. binding relative to IMPβ1

IMPβ1 IMPα2 IMPα2
       WT   ΔIBB
Ei24N

p < 0.05   p < 0.05
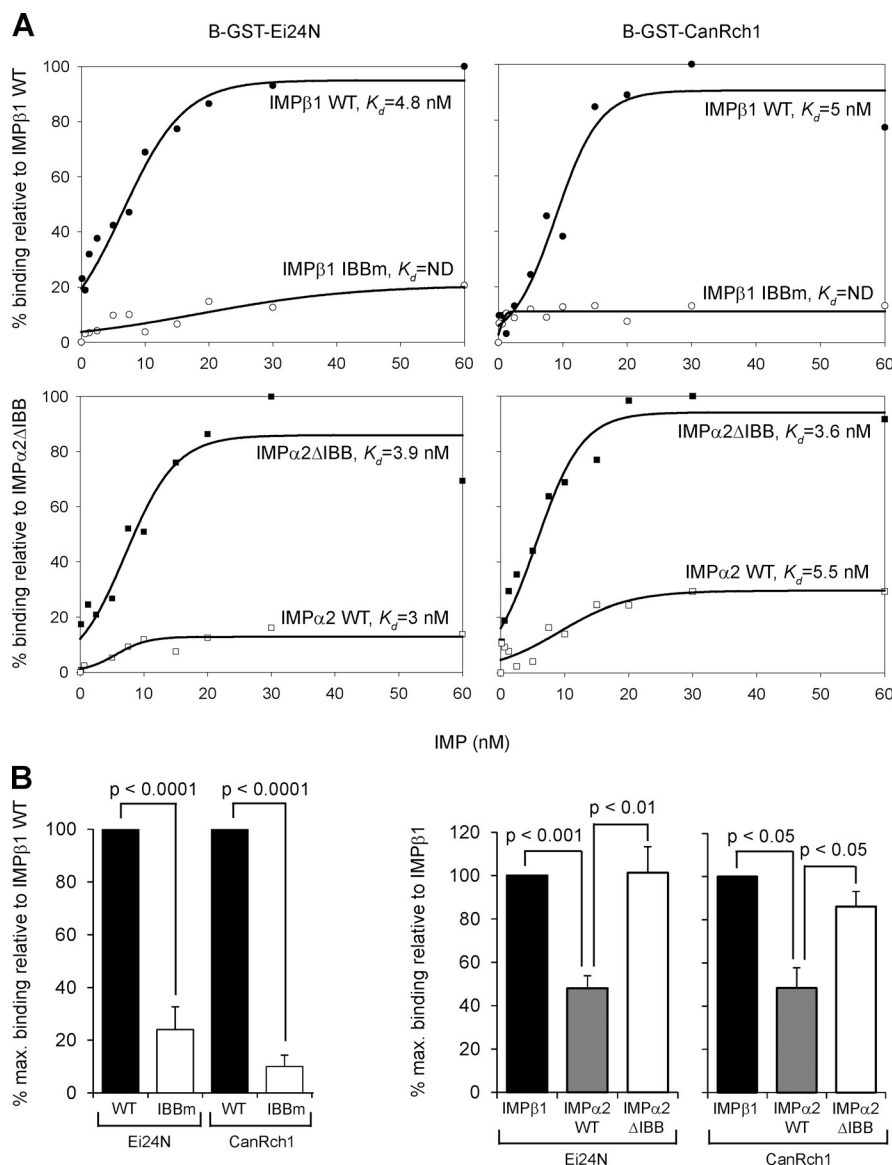
IMPβ1 IMPα2 IMPα2
       WT   ΔIBB
CanRch1

Figure 3. **Like CanRch1, Ei24 can bind directly to IMPβ1 and IMPαΔIBB with high affinity.** (A) 30 nM of biotinylated (B)-GST-Ei24(N) or B-GST-CanRch1 was added to increasing concentrations of IMPβ1 (top), IMPα2 (bottom), or their mutant derivatives, as indicated, and an AlphaScreen assay was performed (see Materials and methods). Results are for a single experiment (representative of three separate assays), with values calculated as the percentage of binding to IMPβ1 WT or IMPα2ΔIBB, with apparent dissociation constants (K_d) indicated. (B) Pooled data represent the mean percentage of maximal binding (±SEM, error bars; $n \geq 3$) to Ei24N/CanRch1 for each IMP relative to that of IMPβ1 WT; p-values are shown for significant differences. IBBm, IBB-binding mutant.

type (WT) was more than twofold lower (Fig. 3 and Table 1). These results concur with previous studies reporting a very similar K_d for binding of the IMPα IBB to either IMPβ1 or IMPα2ΔIBB (Harreman et al., 2003a,b), as well as strongly reduced binding of the IBB to FL compared with IBB-deleted

IMPα (Catimel et al., 2001), which is consistent with FL IMPα's documented autoinhibited state (Kobe, 1999; Harreman et al., 2003a,b; Goldfarb et al., 2004). The comparable K_d of ∼7 nM for the Ei24 IBBL and CanRch1 binding to FL and IBB truncated IMPα2 indicates that the binding site for the

Table 1.   **Binding affinities of Ei24N and CanRch1 to IMPs**

B-GST protein	His-IMP	K_d	B_{max}
		nM	*%*
Ei24N	IMPβ1 WT	5.1 ± 0.6	100 ± 0.06
	IMPβ1 IBBm	ND	24.0 ± 5.0 (P < 0.001)
	IMPα2 WT	7.3 ± 1.4	48.0 ± 5.8 (P < 0.001)
	IMPα2ΔIBB	4.4 ± 2.2	101 ± 12
CanRch1	IMPβ1 WT	4.5 ± 0.5	100 ± 0.2
	IMPβ1 IBBm	ND	10.0 ± 2.5 (P < 0.001)
	IMPα2 WT	6.6 ± 3.5	48.4 ± 9.3 (P < 0.05)
	IMPα2ΔIBB	9.6 ± 2.1	86.2 ± 7.0

Pooled data ($n \geq 3$) from AlphaScreen assays performed as per Fig. 3 for the binding affinities (K_d) and maximal binding (B_{max}) expressed as a percentage of B_{max} relative to IMPβ1 for Ei24N and CanRch1, respectively. Results are for the mean ± SEM, with significant differences in maximal binding relative to IMPβ1 denoted by p-values. Harreman et al. (2003b) showed that binding of the IMPα IBB to IMPβ1 and IMPα2ΔIBB is near identical in terms of K_d.

Ei24 IBBL is the NLS-binding site of IMPα. IMP binding to GST alone was negligible (unpublished data), underlining the specificity of the interactions. All results were consistent with the idea that the Ei24 IBBL can bind directly to IMPβ1, in comparable fashion to the IMPα IBB itself.

Endogenous Ei24 can inhibit p53 nuclear import

To test the effect of high-affinity interaction of Ei24 with IMPs on IMPα2/β1-dependent nuclear import, a p53 WT and knock-out (KO) murine embryonic fibroblast (MEF) system was used together with etoposide treatment (Liang and Clarke, 1999; Kim et al., 2000), which markedly up-regulates Ei24 expression in WT MEFs but not in MEFs lacking p53 (p53 KO; Fig. 4, A and B). GFP-p53 was expressed in DMSO or etoposide-treated p53 WT and KO MEFs (Fig. 4 C), with GFP-aF10(696–794 aa), the nuclear import of which is IMP independent (Cai et al., 2002), and GFP alone as controls. Quantitative analysis to determine the nuclear-to-cytoplasmic fluorescence ratio (Fn/c) revealed that etoposide-treated WT MEFs significantly ($P < 0.005$) reduced (∼60%) the level of GFP-p53 nuclear accumulation compared with in its absence (Fig. 4 D); p53 KO MEFs showed no such effect. Notably, etoposide treatment of WT MEFs increased the number of GFP-p53 cytoplasmic aggregates compared with in its absence (Fig. 4 C), in contrast to KO MEFs, which showed few aggregates, implying that this localization may relate to Ei24 action. No aggregates were observed for the GFP-aF10 or GFP controls, which were unaffected by etoposide treatment (Fig. 4 D), underlining the specificity of the effect. p53-dependent up-regulation of Ei24 in response to etoposide can thus lead to inhibition of IMPα/β1-mediated nuclear accumulation of GFP-p53, which implies that Ei24 may function in a negative feedback loop to contribute to dampening p53 activity in DNA damage (Lohrum et al., 2001; Nie et al., 2007). Reducing p53 nuclear access would in turn stem Ei24 up-regulation and initiate a return to steady state.

We also examined whether ectopically expressed Ei24 could inhibit nuclear accumulation of endogenous p53 in HeLa-Bcl$_{XL}$ cells expressing DsRed2-Ei24 FL or DsRed2-Ei24N, which, because it lacks the C-terminal portion of Ei24 but retains the IBBL, does not localize strongly in the ER, instead being largely nuclear (Fig. 4 E). This is consistent with the idea that like the IMPα IBB, the IBBL can also function as a modular NLS (Görlich et al., 1996a; see also Fig. 5 A for DsRed2-CanRch1). Particular C-terminal sequences and/or the presence of all of the six transmembrane domains are presumably necessary for Ei24 ER targeting, as is the case for other ER proteins (Sato et al., 1996; Honsho et al., 1998; Barré et al., 2005). Cells were fixed 20 h after transfection and immunostained for endogenous p53 or the heterogeneous nuclear ribonucleoprotein hnRNPA1, whose nuclear transport is dependent on IMPβ2 (Nakielny et al., 1996; Fridell et al., 1997; Fig. 4 E). No significant effects on nuclear localization were observed for hnRNPA1, but both DsRed2-Ei24FL and -Ei24N significantly ($P < 0.001$) reduced p53 nuclear accumulation (up to ∼40%) compared with in their absence (Fig. 4 F). The fact that nuclear localized Ei24N retaining the IBBL was capable of inhibiting

p53 nuclear import is consistent with previous observations for CanRch1 (Kim et al., 2000), and implies that the C terminus/ER localization of Ei24 is not essential for inhibition of p53 nuclear import.

Ei24 is a general inhibitor of IMPβ1- and IMPα2/β1-mediated nuclear import

To test the ability of Ei24 to inhibit nuclear protein import generally, DsRed2-Ei24FL and DsRed2-Ei24N were coexpressed with constructs where GFP is fused to either the nuclear targeting signal of chicken anemia virus viral protein 3 (VP3; Wagstaff and Jans, 2006) or telomeric-repeat binding factor TRF1 (Forwood and Jans, 2002), both of which are dependent on IMPβ1 for nuclear import (Fig. 5, A and B; and Fig. S2). Results were compared with those for DsRed2-CanRch1. Although GFP-VP3 was strongly nuclear when expressed alone, increased cytoplasmic fluorescence was evident in cells coexpressing DsRed2-tagged Ei24FL, Ei24N, or CanRch1 (Fig. 5 A), with quantitative analysis confirming a significant ($P < 0.05$) reduction (up to ∼30%) in the Fn/c (Fig. 5 B). A similar trend was observed for GFP-TRF1, which indicates a significant ($P < 0.001$) decrease in the Fn/c in the presence of DsRed2-tagged Ei24FL, Ei24N, or CanRch1, compared with in their absence (Fig. S2).

We also assessed the ability of Ei24 and CanRch1 to inhibit IMPα/β1-mediated nuclear import, observing a significant ($P < 0.0001$) up to ∼65% reduction in the Fn/c for GFP-p53 upon ectopic expression of DsRed2-tagged Ei24FL, Ei24N, or CanRch1 compared with that of GFP-p53 expressed alone (Fig. 5, A and B), with similar results for the prototypical IMPα/β1-recognized cargo GFP-T-ag NLS (Fig. S2). Overexpression of DsRed2-Ei24 or -CanRch1 did not affect nuclear accumulation of GFP-aF10 (Fig. 5, A and B). Collectively, the results indicate that the N terminus of Ei24 is sufficient to inhibit nuclear import specifically mediated by either IMPβ1 alone or IMPα/β1.

A polyarginine sequence within the IBBL domain is required for IMPβ1 binding and nuclear import inhibition

Harreman et al. (2003b) previously reported that mutations to the polybasic "RRRR" motif in the IMPα IBB domain greatly reduce the affinity of binding to IMPβ1; this motif is present within the IBBL domain (RRRR[62]) from mouse and human Ei24 (Fig. 1 C). To test the contribution of these residues to Ei24 binding to IMPβ1, a FLAG-Ei24–encoding construct in which RRRR[62] was mutated to alanine (RRRRm) was tested for its ability to bind IMPβ1 in HEK293T cells compared with that of the comparable WT construct. Whereas FLAG-Ei24 WT clearly interacted with endogenous IMPβ1, the mutant derivative RRRRm (Fig. 5 C) or derivative lacking the entire IBBL domain (not depicted) significantly ($P < 0.0001$) reduced the levels of immunoprecipitated IMPβ1, which indicates that the RRRR motif within the IBBL is required for Ei24 binding to IMPβ1. To assess the effect of the RRRRm mutation on Ei24's ability to inhibit nuclear import, HeLa-Bcl$_{XL}$ cells were transfected to express GFP-p53, -VP3, or -aF10 together with FLAG-Ei24 WT or the mutant derivatives RRRRm or RKQ[79] (RKQm) as a control (Fig. 5, D and E). Nuclear accumulation of
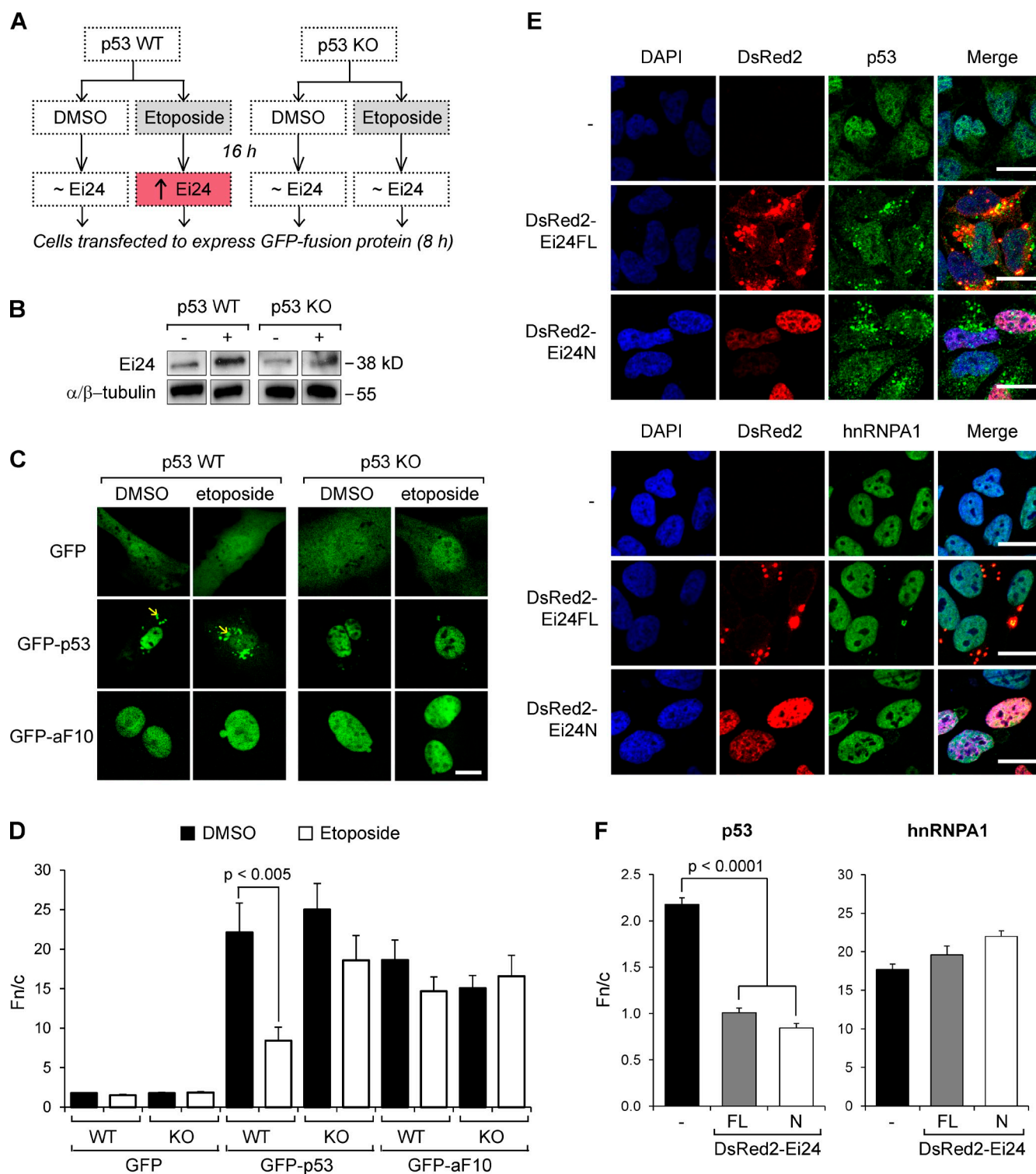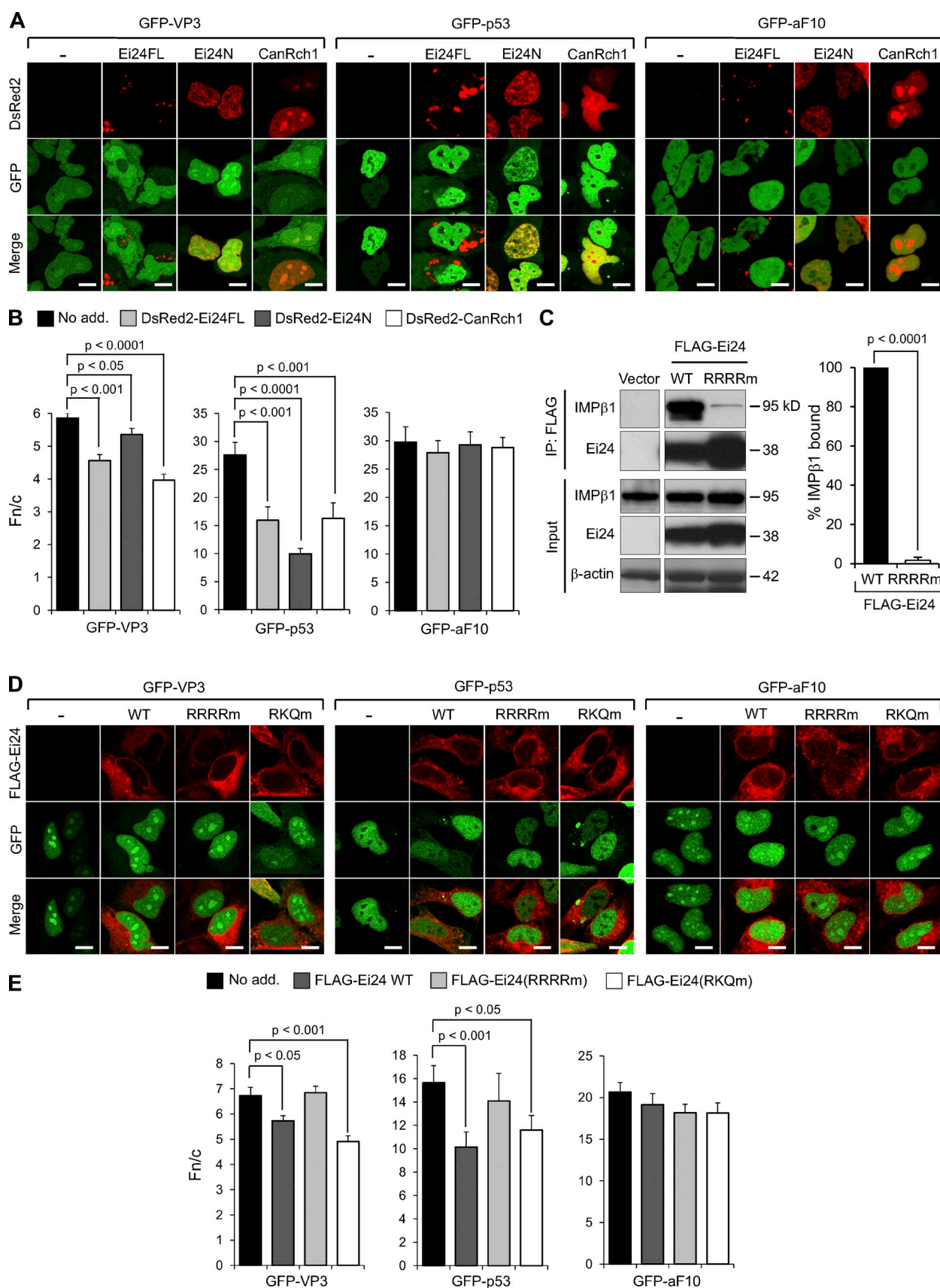
Figure 4. **Ei24 can inhibit nuclear translocation of p53.** (A) Schematic of the experimental layout. (B) Western analysis of lysates from p53 WT and KO MEFs, treated with either 50 µM etoposide or DMSO vehicle control for 16 h, using an anti-Ei24 antibody with α/β-tubulin as a loading control. (C) Cells as in A were imaged live by CLSM 8 h after transfection. Cytoplasmic aggregates of GFP-p53 are indicated by yellow arrows. Bar, 20 µm. (D) Digitized images such as those in C were analyzed to calculate the nuclear-to-cytoplasmic fluorescence ratio (Fn/c; see Materials and methods). Results are for the mean ± SEM (error bars; $n \geq 34$) from a single assay representative of three separate experiments. (E) HeLa-Bcl$_{XL}$ cells transfected to express DsRed2-fusion proteins, as indicated, were fixed 20 h after transfection before immunostaining using specific antibodies for endogenous p53 (top) or hnRNPA1 (bottom), and DAPI counterstaining. Bars, 20 µm. (F) Results from analysis such as that shown in E are for the mean ± SEM (error bars; $n \geq 65$). P-values denote significant differences.

Figure 5. **Ei24 can inhibit IMPβ1- or IMPα2/β1-mediated nuclear accumulation dependent on a polyarginine sequence within its IBBL domain.** (A) Live-cell CLSM images of HeLa-Bcl$_{XL}$ cells transfected to coexpress the indicated GFP and DsRed2 fusion proteins 20 h after transfection. Bars, 10 μm. (B) Quantitative analysis for the extent of nuclear accumulation (Fn/c) of the various GFP fusion proteins. Results are for the mean ± SEM (error bars; $n \geq 41$) from a

the IMPβ1 nuclear import cargo GFP-VP3 was significantly (P < 0.05) reduced by Ei24 WT and the RKQm mutant, in stark contrast to coexpression with RRRRm. Comparably, there was a significant (up to 35%) decrease in the Fn/c of GFP-p53 in the presence of Ei24 WT (P < 0.001) and RKQm (P < 0.05), respectively, but not RRRRm, relative to GFP-p53 alone (Fig. 5, D and E). A similar trend was observed for the IMPα/β1-recognized cargo, GFP-T-ag NLS (Fig. S2). No effect of Ei24 WT, RRRRm, or RKQm was detectable for nuclear accumulation of GFP-aF10, which is consistent with the idea that Ei24 inhibition of nuclear import is specific for IMPα/β1- and IMPβ1-dependent cargoes. Thus, Ei24's conserved RRRR[62] motif, but not RKQ[79], is central to Ei24-dependent inhibition of nuclear import through specific binding to IMPβ1.

In summary, this is the first study to shed light on the function of the ER-localized p53-induced factor Ei24, showing that it possesses a novel IBBL domain that retains key properties of the prototypical IBB of IMPα in terms of ability to bind to IMPβ1, as well as to IMPα, through the same binding site as that used to bind the IBB. Instead of facilitating nuclear import, however, Ei24 inhibits IMPα/β1- and β1-dependent nuclear protein import by sequestering IMPβ1 and possibly IMPα in the cytoplasm/at the ER. We postulate that there is a fine balance between IMP-dependent nuclear import and inhibition thereof by Ei24, enabling fine tuning of the nuclear import efficiency of important proteins such as p53 during normal cell function, as well as during stress such as DNA damage. Perturbation of the balance between these import pathways can clearly be effected by changes in expression of Ei24, as shown here (Fig. 1 D and Fig. 4). Relatively small changes in the cellular pool of IMPβ1 and possibly IMPα can significantly impact the nuclear transport efficiency of key nuclear import cargoes as shown here, and in turn, presumably, autophagy/stress responses and/or apoptosis (Gu et al., 2000).

Increased nuclear IMPα levels have been reported to correlate with poor prognoses for patients with advanced breast cancer (Gluz et al., 2008), with nuclear import specifically enhanced in cancerous/transformed cells (Kuusisto et al., 2012). Clearly, deregulated IMPα/β1-mediated nuclear import is closely linked to tumorigenesis. The role of Ei24 in inhibiting IMP-dependent nuclear protein import in this context may be absolutely critical, as well as the basis of Ei24's tumor suppressor properties, and is the focus of future work in this laboratory.

Materials and methods

Plasmid constructs
FLAG-Ei24 (and mutant derivatives thereof), GFP-Ei24, DsRed2-Ei24, GFP-p53, GFP-VP3, GFP-T-ag NLS, GFP-TRF1, and GFP-aF10 were expressed under the control of a cytomegalovirus (CMV) promoter encoded by mammalian expression constructs prk5-FLAG-Ei24 (and mutant derivatives thereof), prk5-GFP-Ei24, prk5-DsRed2-Ei24, pEPI-GFP-p53, pEPI-GFP-VP3 (residues 74–121), pEGFP-C1-T-ag NLS (residues 111–135), pEPI-GFP-TRF1 (residues 337–440), and pEPI-GFP-aF10 (residues 696–794), respectively (Gu et al., 2000; Kuusisto et al., 2008, 2012; Wagstaff et al., 2012). The pGEX-6P vector plasmids, encoding Ran WT or the mutant derivative Q69L as GST fusion proteins under the control of the tac promoter (Tachibana et al., 2000; Ogawa et al., 2012), were supplied by Y. Miyamoto (Monash University, Clayton, Australia). The N-terminal fragment of Rch1 (residues 2–89), corresponding to a human breast cancer line–derived mutation (Kim et al., 2000) referred to here as CanRch1, was cloned into the pDsRed2-C1 vector (Takara Bio Inc.) using BglII–BamHI sites to produce pDsRed2-C1-CanRch1. To generate pDsRed2-Ei24(2–225) (Ei24N), which corresponds to a truncation mutation in Ei24 derived from a human breast cancer sample (Gentile et al., 2001) and pDEST15-GST-CanRch1, the coding sequences of Ei24N (containing residues 2–225) and CanRch1, respectively, were introduced into the Gateway system (Invitrogen) by PCR using attB site-containing primers and subsequent BP and LR recombination reactions. The integrity of all plasmid constructs was verified by DNA sequencing (Micromon DNA Sequencing Facility, Monash University).

Multiple sequence alignments for the Ei24 IBBL and IMPα IBB domains
Multiple sequence alignment of the human and mouse Ei24 IBBL domains together with the IBB domain from IMPα2/CanRch1 was performed using ClustalW2 (European Molecular Biology Laboratory European Bioinformatics Institute) and BioEdit Sequence Alignment Editor version 7.0.9.0. NCBI protein database accession numbers used for the alignment were: mEi24, *Mus musculus* Ei24 (NP_031941); hEi24, *Homo sapiens* Ei24 (NP_004870); *M. musculus* IMPα2 (AAH03274); and *H. sapiens* Rch1 (EAL24416).

Cell culture and transfection
The HEK293T, HeLa, and HeLa-Bcl$_{XL}$ cell lines were all maintained in DMEM supplemented with 10% FCS, penicillin, and streptomycin in a humidified incubator with 5% CO_2 atmosphere at 37°C. HeLa-Bcl$_{XL}$ cells are resistant to apoptosis induced by Ei24 overexpression (Gu et al., 2000). Cells were transfected at 70–80% confluency using Lipofectamine 2000 (Invitrogen) according to the manufacturer's instructions.

Confocal laser scanning microscopy (CLSM)
Cells were imaged ~16–20 h after transfection on an imaging system (Yokogawa CSU10 based CLSM system; Ultraview; PerkinElmer) with an EM charge-coupled device camera (Andor Technology) and a 100×/1.4 NA oil immersion objective lens (Olympus) or an inverted CLSM system (C1 Inverted; Nikon) using a 100×/1.4 NA oil immersion objective lens (Nikon; Monash Micro Imaging). Cells were imaged in phenol red–free DMEM (Life Technologies), and live-cell imaging was routinely performed on a stage heated to 37°C. The Andor iQ and NIS-Elements version 4.10 software was used for image acquisition on the Ultraview (PerkinElmer) and CLSM (C1 Inverted; Nikon) systems, respectively. Digitized images were subsequently analyzed using the ImageJ 1.33u software (National Institutes of Health) to calculate the nuclear (F_n) to cytoplasmic (F_c) fluorescence ratio ($F_{n/c}$), corrected for by subtracting the background fluorescence (F_b). ImageJ software was also used to alter the brightness and contrast levels uniformly across all samples in the same assay to enhance visibility and for pseudocoloring where appropriate.

Indirect immunofluorescence
Cells were fixed with 4% paraformaldehyde (Sigma-Aldrich) 16–20 h after transfection and permeabilized using 0.2% Triton X-100 (Sigma-Aldrich) in blocking buffer (1% BSA in PBS). Non-specific binding sites were blocked with blocking buffer and immunostained with primary antibodies anti-Ei24 (Ab35) at 1:100, anti-IMPβ1 (Abcam) at 1:500, anti-IMPα2 (BD) at 1:200,

single assay representative of three separate experiments; p-values denote significant differences. (C) Lysates from HEK293T cells transfected to express FLAG-Ei24 WT, RRRRm mutant derivative, or vector alone were subjected to immunoprecipitation using anti-FLAG M2 antibody. Western analysis was performed on input and immunoprecipitates (IP: FLAG) using specific antibodies against IMPβ1 or Ei24, with β-actin as a control. Densitometric analysis was performed on images such as those shown in C; results are for the mean ± SEM (error bars n = 3) for binding (%) relative to that for WT. (D) CLSM images of HeLa-Bcl$_{XL}$ cells transfected to coexpress the indicated GFP fusion proteins in the absence or presence of FLAG-Ei24 derivatives were fixed 20 h after transfection before being immunostained using an anti-FLAG M2 antibody. Bars, 10 µm. (E) Quantitative analysis of the extent of nuclear accumulation for the various GFP fusion proteins. Results shown are for the mean ± SEM (error bars; n ≥ 40) for a single assay representative of three independent experiments. Statistical analysis was performed as in B.

anti-IMP7 (GeneTex) at 1:500, or anti-FLAG M2 (Sigma-Aldrich) at 1:200 for 90 min, followed by a 60-min incubation with Alexa Fluor 488– or Alexa Fluor 568–conjugated secondary antibodies (Molecular Probes) at 1:1,000. Coverslips were mounted onto glass slides with 4% (wt/vol) propyl-gallate in 90% glycerol (Sigma-Aldrich) or ProLong Gold antifade reagent with DAPI mounting media (Molecular Probes). Cells were imaged on the Ultraview or C1 Inverted CLSM systems using a 100×/1.4 NA oil immersion objective lens at room temperature. Digitized images were analyzed and processed using ImageJ software as described in the previous section.

Quantitative colocalization
Colocalization analysis was performed on digitized CLSM images using the ImageJ 1.33u software, where a defined Ei24 threshold signal above background levels (secondary antibody alone control) was overlaid onto that of the IMP signal to produce a merged image for colocalized Ei24 and IMP pixels. The pixel intensity of the merged image was expressed as a percentage of the total IMP signal to calculate the mean percentage of IMP colocalized with Ei24.

Protein expression, purification, and biotin labeling
GST-Ei24N (2–225 aa), GST-CanRch1, and GST-Ran (WT/Q69L; Tachibana et al., 2000; Ogawa et al., 2012) fusion proteins were expressed in *Escherichia coli* strain BL21(DE3) containing a pRARE2 plasmid. Cultures were grown to an OD_{600} of 0.6–1 and protein expression was induced with 0.1–1 mM IPTG for 6 h at 18°C. Pellets were lysed in 50 mM Tris, pH 8.0, 500 mM NaCl, 5 mg/ml lysozyme (Research Organics), and Complete EDTA-free protease inhibitors (Roche) before being sonicated three times for 30 s at 30-s intervals. Protein was purified from cleared lysate with equilibrated glutathione Sepharose 4B resin (GE Healthcare) and incubated at 4°C for 2 h, before elution with 10 mM of reduced gluta-thione in 50 mM Tris, pH 8, and 500 mM NaCl. Glutathione was removed by dialysis and protein concentrated using a Centricon centrifugal filter unit with an appropriate molecular weight cutoff (Amicon; EMD Millipore). For AlphaScreen assays, recombinant GST fusion proteins were labeled using the EZ-Link Sulfo-NHS-LC-LC-Biotin reagent (Thermo Fisher Scientific), and free biotin was separated from labeled protein using a PD-10 Desalting Column (GE Healthcare), according to the manufacturer's instructions. For the GST-Ran WT and GST-Ran(Q69L) proteins, GST was removed using PreScission Protease (GE Healthcare) according to manufacturer's instructions, and the proteins then loaded with GDP or GTPγS (Sigma-Aldrich), respectively, as described previously (Tachibana et al., 2000).

Hexa-histidine (His₆)-tagged full-length IMPα2 and IMPαΔIBB (residues 67–503; Yang et al., 2010) were provided by S. Yang (Monash University). In brief, protein was expressed in *E. coli* strain BL21(DE3) grown to an OD_{600} of 1.0 and induced with 1 mM IPTG for 4 h at 28°C. Proteins were purified by affinity chromatography using nickel-nitrilotriacetic acid agarose (QIAGEN) and eluted in 500 mM imidazole. Dialysis was performed to remove imidazole. His₆-IMPβ1 WT and IBBm (containing mutations W430A/W472A/W864A) proteins were expressed in the *E. coli* ER1003 strain and purification was performed on chitin beads followed by gel filtration on a Superose-12 column as described previously (Koerner et al., 2003).

AlphaScreen binding assay
The binding affinity of biotinylated GST-Ei24N, GST-CanRch1 or GST alone to His₆-tagged IMPs was determined using the bead-based AlphaScreen assay (PerkinElmer), as described previously (Wagstaff and Jans, 2006). In brief, 30 nM of biotinylated GST-Ei24N, GST-CanRch1, or GST alone was incubated with increasing concentrations of His₆-tagged IMPs. After incubation with nickel-chelating acceptor and streptavidin-coated donor beads, results were read on a Fusionα plate reader (PerkinElmer). Triplicate values were averaged and sigmoidal titration curves (three-parameter sigmoidal fit) were plotted using the SigmaPlot graphing program (Systat Software Inc.) to determine the dissociation constant (K_d) and maximal binding (B_{max}) value. It should be noted that the sensitivity of the AlphaScreen binding assay results in lower estimated K_d values than various other assays (e.g., Catimel et al., 2001; Forwood and Jans, 2002; Harreman et al., 2003a,b; Fulcher et al., 2010), but relative/comparative values are comparable (e.g., see the legend for Table 1).

Immunoprecipitation and Western analysis
For IP of endogenous Ei24, HEK293T cells grown in 10-cm² dishes were lysed in RIPA buffer (50 mM Tris-HCl, 100 mM NaCl, 2 mM EDTA, 50 mM NaF, 0.4% sodium deoxycholate, 1% Triton X-100, and 1× Complete EDTA-free protease inhibitors) and passed through a 26-gauge syringe

10 times. Precleared lysate was added to 10 µg anti-Ei24 (Sigma-Aldrich) or rabbit IgG (Santa Cruz Biotechnology, Inc.) antibody and 50 µl Protein A/G plus agarose slurry (Santa Cruz Biotechnology, Inc.), and incubated overnight at 4°C. Immunoprecipitates were washed with RIPA buffer and eluted in 3× Laemmli sample buffer. HeLa-Bcl$_{XL}$ cells grown in 6-cm² dishes expressing GFP-Ei24 or GFP-IMPβ1 fusion proteins were lysed with dilution buffer (20 mM Tris-HCl, pH 7.5, 150 mM NaCl, and 0.5 mM EDTA), 0.5% NP-40 (Sigma-Aldrich), and Complete EDTA-free protease inhibitors (Roche). In some experiments, lysates were preincubated with a final concentration of 1.7 mM GTPγS (Sigma-Aldrich) or 3 µM recombinant Ran reconstituted with GTPγS or GDP for 20 min on ice. Immunocomplexes were bound to and eluted from the GFP-Trap resin (ChromoTek) according to the manufacturer's instructions. Protein from whole-cell extracts or immunoprecipitates were resolved by SDS-PAGE and transferred to nitrocellulose membrane (Pall). Specific proteins were detected on membranes probed with anti-GFP (Roche) at 1:1,000, anti-IMPβ1 (provided by D. Görlich,, Max Planck Institute, Göttingen, Germany; or from Abcam) at 1:1,000, anti-IMPα4 (KPNA3; Abcam) at 1:500, anti-IMPα2 (BD) at 1:1,000, anti-IMPβ2 (BD) at 1:500, anti-IMP13 (rabbit polyclonal antibody generated against the synthetic peptides LPEEFQTSRLPQYRKGLVR and EQKDTF-SQQILRERVNKRRVK; Tao et al., 2006) at 1:1,000, anti-FLAG antibody (Sigma-Aldrich), or anti-BiP (Cell Signaling Technology), together with species-specific HRP-conjugated secondary antibody (EMD Millipore). Protein bands were visualized using Western Lightning ECL reagent (PerkinElmer) and chemiluminescence detection on x-ray film (Fujifilm). Densitometric analysis of protein bands was performed on digitized images of immunoblots using the ImageJ 1.33u software (Kaur et al., 2013).

Mass spectrometry (MS)
Immunoprecipitated proteins transferred to nylon membranes were identified by Sypro Ruby Protein Gel Stain (Molecular Probes; Life Technologies), excised, reduced, and alkylated with iodoacetamide, and digested with trypsin. The unfractionated tryptic digest was subjected to MS using the 4700 Proteomics Analyzer (Applied Biosystems), which employs matrix-assisted laser desorption/ionization (MALDI) in conjunction with tandem time-of-flight (TOF) mass analyzers. The digest was introduced into the instrument in a crystalline matrix of α-cyano-4-hydroxycinnamic acid. Database searches were performed with GPS Explorer software (Applied Biosystems), using the Mascot search engine (Perkins et al., 1999). Protein assignments were made based on both the MS and MS/MS spectra. Top-ranking proteins that had a significant ($P < 0.05$) Mascot score from each band were identified (see Table S1 for detailed analyses). The protein scores were derived from ions scores as a nonprobabilistic basis for ranking protein hits. The Swiss-Prot database was used for protein identification.

Membrane topology analysis
Membrane topology for Ei24 was assessed using a modified method as described previously (Leighton and Schatz, 1995). In brief, cell pellets from N-terminally FLAG-tagged Ei24 transfected HEK293 cells were washed with cold 1× PBS and resuspended in buffer A (10 µM NaCl, 1.5 µM MgCl$_2$, and 10 µM Tris, pH 7.5, containing complete proteinase inhibitor cocktail) for 1 h on ice. Cells were homogenized with a type B Dounce homogenizer until 80% of cells were lysed. An equal volume of buffer B (210 µM mannitol, 70 µM sucrose, 5 µM Tris, pH 7.5, and 1 µM EDTA, pH 7.5) was added immediately and the lysate was centrifuged at 700 *g* for 10 min at 4°C to remove nuclei/intact cells. The supernatant was transferred into a new tube and then centrifuged at 1,200 *g* for 15 min at 4°C to isolate ER pellets, which were then resuspended in buffer B and aliquoted in 200-µg protein amounts. ER fractions were incubated for 30 min on ice in the presence or absence of 1 mg/ml proteinase K and inactivated using cold trichloroacetic acid. After centrifugation, the fractions were analyzed by Western blotting (as described earlier in the Materials and methods).

Online supplemental material
Fig. S1 (A and B) shows proteomic analysis of FLAG-Ei24 immunoprecipitates with a preimmune antibody control and Ei24's topology at the ER, with Table S1 showing MS analysis details. Fig. S1 (C and D) shows quantitative colocalization analysis of Ei24 and IMPs in etoposide-treated HeLa cells. Fig. S2 demonstrates that Ei24 can inhibit IMPβ1- and IMPα2/β1-mediated nuclear translocation of GFP-TRF1 and -T-ag NLS, respectively. Online supplemental material is available at http://www.jcb.org/cgi/content/full/jcb.201304055/DC1.

References

Barré, L., J. Magdalou, P. Netter, S. Fournel-Gigleux, and M. Ouzzine. 2005. The stop transfer sequence of the human UDP-glucuronosyltransferase 1A determines localization to the endoplasmic reticulum by both static retention and retrieval mechanisms. *FEBS J.* 272:1063–1071. http://dx.doi.org/10.1111/j.1742-4658.2005.04548.x

Bergqvist, S., C.H. Croy, M. Kjaergaard, T. Huxford, G. Ghosh, and E.A. Komives. 2006. Thermodynamics Reveal That Helix Four in the NLS of NF-κB p65 Anchors IκBα, Forming a Very Stable Complex. *J. Mol. Biol.* 360:421–434. http://dx.doi.org/10.1016/j.jmb.2006.05.014

Cai, Y., Y. Gao, Q. Sheng, S. Miao, X. Cui, L. Wang, S. Zong, and S.S. Koide. 2002. Characterization and potential function of a novel testis-specific nucleoporin BS-63. *Mol. Reprod. Dev.* 61:126–134. http://dx.doi.org/10.1002/mrd.1139

Catimel, B., T. Teh, M.R.M. Fontes, I.G. Jennings, D.A. Jans, G.J. Howlett, E.C. Nice, and B. Kobe. 2001. Biophysical characterization of interactions involving importin-α during nuclear import. *J. Biol. Chem.* 276:34189–34198. http://dx.doi.org/10.1074/jbc.M103531200

Cingolani, G., C. Petosa, K. Weis, and C.W. Müller. 1999. Structure of importin-β bound to the IBB domain of importin-α. *Nature.* 399:221–229. http://dx.doi.org/10.1038/20367

Cingolani, G., J. Bednenko, M.T. Gillespie, and L. Gerace. 2002. Molecular basis for the recognition of a nonclassical nuclear localization signal by importin β. *Mol. Cell.* 10:1345–1353. http://dx.doi.org/10.1016/S1097-2765(02)00727-X

Conti, E., and J. Kuriyan. 2000. Crystallographic analysis of the specific yet versatile recognition of distinct nuclear localization signals by karyopherin α. *Structure.* 8:329–338. http://dx.doi.org/10.1016/S0969-2126(00)00107-6

Ding, Q., S.i. Fukami, X. Meng, Y. Nishizaki, X. Zhang, H. Sasaki, A. Dlugosz, M. Nakafuku, and C. Hui. 1999. Mouse suppressor of fused is a negative regulator of sonic hedgehog signaling and alters the subcellular distribution of Gli1. *Curr. Biol.* 9:1119–1122. http://dx.doi.org/10.1016/S0960-9822(99)80482-5

Forwood, J.K., and D.A. Jans. 2002. Nuclear import pathway of the telomere elongation suppressor TRF1: inhibition by importin α. *Biochemistry.* 41:9333–9340. http://dx.doi.org/10.1021/bi025548s

Fridell, R.A., R. Truant, L. Thorne, R.E. Benson, and B.R. Cullen. 1997. Nuclear import of hnRNP A1 is mediated by a novel cellular cofactor related to karyopherin-beta. *J. Cell Sci.* 110:1325–1331.

Fulcher, A.J., D.M. Roth, S. Fatima, G. Alvisi, and D.A. Jans. 2010. The BRCA-1 binding protein BRAP2 is a novel, negative regulator of nuclear import of viral proteins, dependent on phosphorylation flanking the nuclear localization signal. *FASEB J.* 24:1454–1466. http://dx.doi.org/10.1096/fj.09-136564

Gentile, M., M. Ahnström, F. Schön, and S. Wingren. 2001. Candidate tumour suppressor genes at 11q23-q24 in breast cancer: evidence of alterations in PIG8, a gene involved in p53-induced apoptosis. *Oncogene.* 20:7753–7760. http://dx.doi.org/10.1038/sj.onc.1204993

Gluz, O., P. Wild, R. Meiler, R. Diallo-Danebrock, E. Ting, S. Mohrmann, G. Schuett, E. Dahl, T. Fuchs, A. Herr, et al. 2008. Nuclear karyopherin α2 expression predicts poor survival in patients with advanced breast cancer irrespective of treatment intensity. *Int. J. Cancer.* 123:1433–1438. http://dx.doi.org/10.1002/ijc.23628

Goldfarb, D.S., A.H. Corbett, D.A. Mason, M.T. Harreman, and S.A. Adam. 2004. Importin α: a multipurpose nuclear-transport receptor. *Trends Cell Biol.* 14:505–514. http://dx.doi.org/10.1016/j.tcb.2004.07.016

Görlich, D., P. Henklein, R.A. Laskey, and E. Hartmann. 1996a. A 41 amino acid motif in importin-α confers binding to importin-β and hence transit into the nucleus. *EMBO J.* 15:1810–1817.

Görlich, D., N. Panté, U. Kutay, U. Aebi, and F.R. Bischoff. 1996b. Identification of different roles for RanGDP and RanGTP in nuclear protein import. *EMBO J.* 15:5584–5594.

Gu, Z., C. Flemington, T. Chittenden, and G.P. Zambetti. 2000. ei24, a p53 response gene involved in growth suppression and apoptosis. *Mol. Cell. Biol.* 20:233–241. http://dx.doi.org/10.1128/MCB.20.1.233-241.2000

Harreman, M.T., P.E. Cohen, M.R. Hodel, G.J. Truscott, A.H. Corbett, and A.E. Hodel. 2003a. Characterization of the auto-inhibitory sequence within the N-terminal domain of importin α. *J. Biol. Chem.* 278:21361–21369. http://dx.doi.org/10.1074/jbc.M301114200

Harreman, M.T., M.R. Hodel, P. Fanara, A.E. Hodel, and A.H. Corbett. 2003b. The auto-inhibitory function of importin α is essential in vivo. *J. Biol. Chem.* 278:5854–5863. http://dx.doi.org/10.1074/jbc.M210951200

Honsho, M., J.Y. Mitoma, and A. Ito. 1998. Retention of cytochrome b5 in the endoplasmic reticulum is transmembrane and luminal domain-deendent. *J. Biol. Chem.* 273:20860–20866. http://dx.doi.org/10.1074/jbc.273.33.20860

Jacobs, M.D., and S.C. Harrison. 1998. Structure of an IκBα/NF-κB complex. *Cell.* 95:749–758. http://dx.doi.org/10.1016/S0092-8674(00)81698-0

Kaur, G., K.G. Lieu, and D.A. Jans. 2013. 70-kDa heat shock cognate protein hsc70 mediates calmodulin-dependent nuclear import of the sex-determining factor SRY. *J. Biol. Chem.* 288:4148–4157. http://dx.doi.org/10.1074/jbc.M112.436741

Kim, I.-S., D.-H. Kim, S.-M. Han, M.-U. Chin, H.-J. Nam, H.-P. Cho, S.-Y. Choi, B.-J. Song, E.-R. Kim, Y.-S. Bae, and Y.-H. Moon. 2000. Truncated form of importin α identified in breast cancer cell inhibits nuclear import of p53. *J. Biol. Chem.* 275:23139–23145. http://dx.doi.org/10.1074/jbc.M909256199

Kobe, B. 1999. Autoinhibition by an internal nuclear localization signal revealed by the crystal structure of mammalian importin α. *Nat. Struct. Biol.* 6:388–397. http://dx.doi.org/10.1038/7625

Koerner, C., T. Guan, L. Gerace, and G. Cingolani. 2003. Synergy of silent and hot spot mutations in importin β reveals a dynamic mechanism for recognition of a nuclear localization signal. *J. Biol. Chem.* 278:16216–16221. http://dx.doi.org/10.1074/jbc.M301137200

Kuusisto, H.V., K.M. Wagstaff, G. Alvisi, and D.A. Jans. 2008. The C-terminus of apoptin represents a unique tumor cell-enhanced nuclear targeting module. *Int. J. Cancer.* 123:2965–2969. http://dx.doi.org/10.1002/ijc.23884

Kuusisto, H.V., K.M. Wagstaff, G. Alvisi, D.M. Roth, and D.A. Jans. 2012. Global enhancement of nuclear localization-dependent nuclear transport in transformed cells. *FASEB J.* 26:1181–1193. http://dx.doi.org/10.1096/fj.11-191585

Lee, S.J., Y. Matsuura, S.M. Liu, and M. Stewart. 2005. Structural basis for nuclear import complex dissociation by RanGTP. *Nature.* 435:693–696. http://dx.doi.org/10.1038/nature03578

Lehar, S.M., M. Nacht, T. Jacks, C.A. Vater, T. Chittenden, and B.C. Guild. 1996. Identification and cloning of EI24, a gene induced by p53 in etoposide-treated cells. *Oncogene.* 12:1181–1187.

Leighton, J., and G. Schatz. 1995. An ABC transporter in the mitochondrial inner membrane is required for normal growth of yeast. *EMBO J.* 14:188–195.

Li, S., C.-Y. Ku, A.A. Farmer, Y.-S. Cong, C.-F. Chen, and W.-H. Lee. 1998. Identification of a novel cytoplasmic protein that specifically binds to nuclear localization signal motifs. *J. Biol. Chem.* 273:6183–6189. http://dx.doi.org/10.1074/jbc.273.11.6183

Liang, S.-H., and M.F. Clarke. 1999. A bipartite nuclear localization signal is required for p53 nuclear import regulated by a carboxyl-terminal domain. *J. Biol. Chem.* 274:32699–32703. http://dx.doi.org/10.1074/jbc.274.46.32699

Lohrum, M.A.E., D.B. Woods, R.L. Ludwig, E. Bálint, and K.H. Vousden. 2001. C-terminal ubiquitination of p53 contributes to nuclear export. *Mol. Cell. Biol.* 21:8521–8532. http://dx.doi.org/10.1128/MCB.21.24.8521-8532.2001

Nakielny, S., M.C. Siomi, H. Siomi, W.M. Michael, V. Pollard, and G. Dreyfuss. 1996. Transportin: nuclear transport receptor of a novel nuclear protein import pathway. *Exp. Cell Res.* 229:261–266. http://dx.doi.org/10.1006/excr.1996.0369

Nie, L., M. Sasaki, and C.G. Maki. 2007. Regulation of p53 nuclear export through sequential changes in conformation and ubiquitination. *J. Biol. Chem.* 282:14616–14625. http://dx.doi.org/10.1074/jbc.M610515200

Ogawa, Y., Y. Miyamoto, M. Oka, and Y. Yoneda. 2012. The interaction between importin-α and Nup153 promotes importin-α/β-mediated nuclear import. *Traffic.* 13:934–946. http://dx.doi.org/10.1111/j.1600-0854.2012.01367.x

Perkins, D.N., D.J.C. Pappin, D.M. Creasy, and J.S. Cottrell. 1999. Probability-based protein identification by searching sequence databases using mass spectrometry data. *Electrophoresis*. 20:3551–3567. http://dx.doi.org/10.1002/(SICI)1522-2683(19991201)20:18<3551::AID-ELPS3551>3.0.CO;2-2

Polyak, K., Y. Xia, J.L. Zweier, K.W. Kinzler, and B. Vogelstein. 1997. A model for p53-induced apoptosis. *Nature*. 389:300–305. http://dx.doi.org/10.1038/38525

Poon, I.K.H., and D.A. Jans. 2005. Regulation of nuclear transport: central role in development and transformation? *Traffic*. 6:173–186. http://dx.doi.org/10.1111/j.1600-0854.2005.00268.x

Sato, M., K. Sato, and A. Nakano. 1996. Endoplasmic reticulum localization of Sec12p is achieved by two mechanisms: Rer1p-dependent retrieval that requires the transmembrane domain and Rer1p-independent retention that involves the cytoplasmic domain. *J. Cell Biol.* 134:279–293. http://dx.doi.org/10.1083/jcb.134.2.279

Tachibana, T., M. Hieda, Y. Miyamoto, S. Kose, N. Imamoto, and Y. Yoneda. 2000. Recycling of importin α from the nucleus is suppressed by loss of RCC1 function in living mammalian cells. *Cell Struct. Funct.* 25:115–123. http://dx.doi.org/10.1247/csf.25.115

Tao, T., J. Lan, G.L. Lukacs, R.J.G. Haché, and F. Kaplan. 2006. Importin 13 regulates nuclear import of the glucocorticoid receptor in airway epithelial cells. *Am. J. Respir. Cell Mol. Biol.* 35:668–680. http://dx.doi.org/10.1165/rcmb.2006-0073OC

Tian, Y., Z. Li, W. Hu, H. Ren, E. Tian, Y. Zhao, Q. Lu, X. Huang, P. Yang, X. Li, et al. 2010. *C. elegans* screen identifies autophagy genes specific to multicellular organisms. *Cell*. 141:1042–1055. http://dx.doi.org/10.1016/j.cell.2010.04.034

Wagstaff, K.M., and D.A. Jans. 2006. Intramolecular masking of nuclear localization signals: analysis of importin binding using a novel AlphaScreen-based method. *Anal. Biochem.* 348:49–56. http://dx.doi.org/10.1016/j.ab.2005.10.029

Wagstaff, K.M., H. Sivakumaran, S.M. Heaton, D. Harrich, and D.A. Jans. 2012. Ivermectin is a specific inhibitor of importin α/β-mediated nuclear import able to inhibit replication of HIV-1 and dengue virus. *Biochem. J.* 443:851–856. http://dx.doi.org/10.1042/BJ20120150

Yang, S.N.Y., A.A.S. Takeda, M.R.M. Fontes, J.M. Harris, D.A. Jans, and B. Kobe. 2010. Probing the specificity of binding to the major nuclear localization sequence-binding site of importin-α using oriented peptide library screening. *J. Biol. Chem.* 285:19935–19946. http://dx.doi.org/10.1074/jbc.M109.079574

Zhao, X., R.E. Ayer, S.L. Davis, S.J. Ames, B. Florence, C. Torchinsky, J.S. Liou, L. Shen, and R.A. Spanjaard. 2005. Apoptosis factor EI24/PIG8 is a novel endoplasmic reticulum-localized Bcl-2-binding protein which is associated with suppression of breast cancer invasiveness. *Cancer Res.* 65:2125–2129. http://dx.doi.org/10.1158/0008-5472.CAN-04-3377

Zhao, Y.G., H. Zhao, L. Miao, L. Wang, F. Sun, and H. Zhang. 2012. The p53-induced gene Ei24 is an essential component of the basal autophagy pathway. *J. Biol. Chem.* 287:42053–42063. http://dx.doi.org/10.1074/jbc.M112.415968